

# High Performance of Unified Power Quality Conditioner and Battery Energy Storage Supplied by Photovoltaic Using Artificial Intelligent Controller

Amirullah<sup>1</sup>, Ontoseno Penangsang<sup>2</sup>, Adi Soeprijanto<sup>2</sup>

**Abstract** – This paper proposes the use of Battery Energy Storage (BES) on an Unified Power Quality Conditioner (UPQC) supplied by Photovoltaic (PV) through DC link to improve power quality on a three-phase three-wire (3P3W) distribution system. The BES serves to store the excess of power resulted by PV and to transfer it to load if necessary, preventing voltage interruption, and adjusting charging and discharging energy in battery. Power quality analysis is carried out in two conditions i.e. PV connected to DC link without and with BES. Fuzzy Logic Controller (FLC) is implemented to maintain DC voltage across the capacitor under disturbance scenarios of source and load as well as to compare the results with Proportional Integral (PI) controller. The number of disturbance scenarios is six for each UPQC controller, so the total number of disturbances is 12. The six disturbances are: non-linear load (NL), unbalance and nonlinear load (Unba-NL), distortion supply and non-linear load (Dis-NL), sag and non-linear load (Sag-NL), swell and non-linear load (Swell-NL), and interruption and non-linear load (Inter-NL). FLC method on UPQC supplied by PV with BES is able to result in an average THD of load voltage slightly better than PI controller. In disturbance scenario 1 to 5, nominal of average THD of load voltage have met IEEE 519. FLC method on UPQC supplied by PV with BES is also capable to give average THD of source current better than PI controller. Under scenario 6 (Inter-NL), FLC is able to reduce the average THD of load voltage and source current significantly than PI controller. With the same disturbance, the combination of PV and BES is able to generate power to UPQC DC link and to inject full average compensation voltage through injection transformer on series active filter so that average load voltage remains stable. This simulations prove that the proposed artificial intelligent (AI) controller for UPQC with BES is able to improve power quality significantly under varying disturbances especially for interruption disturbance. The performance of the proposed model is validated and investigated through simulations using Matlab/Simulink. Copyright © 2018 Praise Worthy Prize S.r.l. - All rights reserved.

**Keywords:** Power Quality, UPQC, PV, BES, Total Harmonic Distortion (THD), Disturbance Scenarios

## Nomenclature

$I_{PV}$	Photovoltaic current	$p$	Real power
$I_o$	Saturated reverse current	$q$	Imaginary power
$N_s$	Number of series cells	$\bar{p}$	Direct component of real power
$q$	Electron charge	$\tilde{p}$	Fluctuating component of real power
$K$	Boltzmann constant	$\bar{q}$	Direct component of imaginary power
$T$	Temperature of p–n junction	$\tilde{q}$	Fluctuating component of imaginary power
$I_{SC}$	Short circuit current	$\bar{p}_{loss}$	Instantaneous active power corresponds to resistive loss and switching loss of UPQC
$V_{OC}$	Open circuit voltage	$i_{c\alpha\beta}^*$	Compensating currents in cartesian $\alpha\beta$
$V_m$	Peak magnitude of fundamental input voltage	$i_{sabc}^*$	Reference source currents in $abc$
$V_{Labc}^*$	Reference load voltages in $abc$	$i_{sabc}$	Sensed source currents in $abc$
$V_{Labc}$	Sensed load voltages in $abc$	$V_{dc}$	Dc link voltage
$V_{abc}$	Voltages in cartesian $abc$	$V_{LL}$	Line-line grid voltage
$I_{abc}$	Currents in cartesian $abc$	$m$	Modulation index
$V_{\alpha\beta}$	Voltages in cartesian $\alpha\beta$	$K_p$	Proportional gain constant
$I_{\alpha\beta}$	Currents in cartesian $\alpha\beta$		

$K_i$	Integral gain constant
$V_{dc-error}$	Error $V_{dc}$
$\Delta V_{dc-error}$	Delta error $V_{dc}$
$V_S$	Source voltage
$V_L$	Load voltage
$I_S$	Source current
$I_L$	Load current
$V_c$	Compensation voltage
THD	Total harmonic distortion
PCC	Point common coupling

## I. Introduction

The microgrid power systems use distributed generations (DGs) power source where power is supplied to local loads and it may operate separately from conventional grid systems [1]-[18]. DGs have many benefits: for example, it is capable of reducing transmission costs, it has low investment costs, it reduces line losses and it increases grid reliability. DGs that use renewable energy (RE) able to generate electrical power are classified as DGs sources. The solar or photovoltaic (PV) generator is one of the most potential DGs sources technologies because it only needs sunlight to generate electricity, where the resources are available in abundance, they are free and relatively clean. Indonesia has an enormous energy potential from the sun because it lies on the equator. Almost all areas of Indonesia get sunlight about 10 to 12 hours per day, with an average intensity of irradiation of 4.5 kWh/m<sup>2</sup> or equivalent to 112,000 GW.

Even though PV generator is capable to generate power, it also has a weakness: it produces a number of voltage and current disturbances, as well as harmonics due to the presence of several types of PV devices and power converters as well as increasing a number of non-linear loads connected to the grid causing a decrease in power quality.

In order to overcome this problem and to improve power quality due to presence of non-linear loads and integration of PV generator to grid, UPQC is proposed [19]. UPQC serves to compensate problems of source voltage quality, for example sag, swell, unbalance, flicker, harmonics, as well as problems of load current quality such as harmonics, unbalance, reactive currents, and neutral currents. UPQC is part of the active power filter consisting of shunt and series active power filters connected in parallel and it serves as a superior controller to overcome a number of power quality problems simultaneously [1]. UPQC series component is responsible to reduce a number of interference on source side; voltage sag/swell, flicker, unbalanced voltage, and harmonics. This equipment serves to inject a number of voltages to keep load voltage fixed at the desired level in a balanced and distortion free. UPQC shunt component is responsible for addressing current quality problem: low power factor, load current harmonics, and unbalanced load. This device serves to inject current on AC system so that source current becomes sinusoidal balanced and in

phase with source voltage [2].

UPQC based on RE has been investigated by many researchers. There are two methods used to overcome the problem by using conventional and artificial intelligence controller. [3] deals with the analysis of UPQC and DG combination operations. The proposed system includes a series inverter, shunt inverter, and a DG connected to a DC link through a rectifier using PI controller. The system has been capable to increase source voltage quality (sag and interruption) and load current quality, as well as to change in active power on grid and off grid mode. The influence of DG on UPQC performance in reducing the sag voltage under conditions of some phase to ground faults to using distributed static compensator (DSTATCOM) controller has been implemented [4]. The DG has been effective enough to help UPQC work in improving sag voltage. DG system is connected in series with load resulting to have a better percentage of sag mitigation compared to the system without using DG.

The implementation of UPQC using unit vector template generation (UVTG) method with PI controller to improve sag, swell, voltage harmonics and current harmonics has been done [5]. The simulation of voltage distortion has been made by adding 5<sup>th</sup> and 7<sup>th</sup> harmonics at fundamental source voltage, resulting in a reduction of THD source current and THD load voltage.

UPQC supplied by a 64 panels PV using boost converter, PI controller, perturb and observer MPPT, and instantaneous reactive power theory (p-q theory) has been proposed [6]. The system has been capable to compensate reactive power and reduce source current and load voltage harmonics. Nevertheless, the study has not discussed the mitigation of sag and interruption caused by penetration of PV. Artificial neural network (ANN) based synchronous reference frame theory (SRF) control strategy to compensate power quality issues in three phase three wire (3P3W) distribution system through UPQC for various balanced/unbalance/distorted conditions on load and source has been proposed [7]. The proposed model has been able to mitigate harmonic/reactive currents, unbalanced source and load current/voltage. Investigation on power quality enhancement includes sag and source voltage harmonics on grid using UPQC supplied by PV array connected to DC link using PI compared with FLC have been done [8]. The simulation shows that FLC on UPQC and PV can improve source voltage THD better than PI.

[9] shows a method to balance current and line voltage, as a result of DGs of a single phase PV generator unit randomly installed in houses through a three-phase four-wire 220 kV and 50 Hz distribution line using BES and three single-phase bidirectional inverters. Both devices have been capable to reduce unbalanced line current and unbalanced line voltage. Both combinations have also been able to increase current and voltage harmonics on PCC bus. Improvement of power quality UPQC on microgrid supplied by PV and wind turbine has been implemented. PI and FLC are able to improve power quality and to reduce distortion in output power

[10].

This research investigates the use of BES on UPQC supplied by PV through to DC link to improve power quality on three-phase three-wire (3P3W) distribution system. PV array generates power under constant temperature and irradiance, connected to BES through a DC/DC boost converter that serves to regulate PV operating point. BES serves to store excess energy produced by PV and to distribute it to load if necessary, in order to prevent interruption voltage, and to adjust charging and discharging of energy in battery. BES is also expected to store excess power produced by PV generator, using them as backup power. FLC is proposed and compared with PI method, because PI controller is weak in determining proportional and integral gain constant which still uses trial and error. FLC is used as a controller variable of DC voltage and DC reference voltage input to generate reference current source in current hysteresis controller circuit on shunt active filter. FLC methods are used as DC voltage controllers in shunt active filter and series active filter to mitigate power quality of load voltage and source current. The number of disturbance scenario is six for each UPQC controller, so the total number is 12. The power quality performance of two controllers are used to determine load voltage, source current, load voltage THD, and source current THD based on IEEE 519.

Section II describes the proposed method, the model of UPQC supplied by PV and BES, the simulation parameters, the PV circuit model, the control of series and shunt active filter, as well as the application of PI

and FLC method for the proposed model. Section III shows the results and the discussion about THD analysis on the proposed model of PV connected to DC link circuit without and with BES using PI controller and FLC.

In this section, six disturbance scenarios are presented and the results are verified with Matlab/Simulink.

Finally, the paper is concluded in Section IV.

## II. Proposed Method

### II.1. Proposed Model

Fig. 1 shows the model proposed in this study. DG based on RE is a PV connected to a 3P3W distribution system with 380 volts (L-L) and a frequency of 50 hertz, through DC link UPQC and BES circuit. PV array generates power under fixed temperature and irradiance and it is connected to BES through a DC/DC boost converter. The maximum power point tracking (MPPT) method with Perturb and Observer (P and O) algorithms helps PV to generate the maximum power and to generate an output voltage, as an input voltage for the DC/DC boost converter. The converter functions to adjust duty cycle value and output voltage of PV generator as its input voltage to produce output voltage according DC link voltage of UPQC.

The BES connected to UPQC DC link circuit serves as an energy storage and it is expected to overcome voltage interruption and to help UPQC performance to enhance voltage and current power quality at source and load bus.

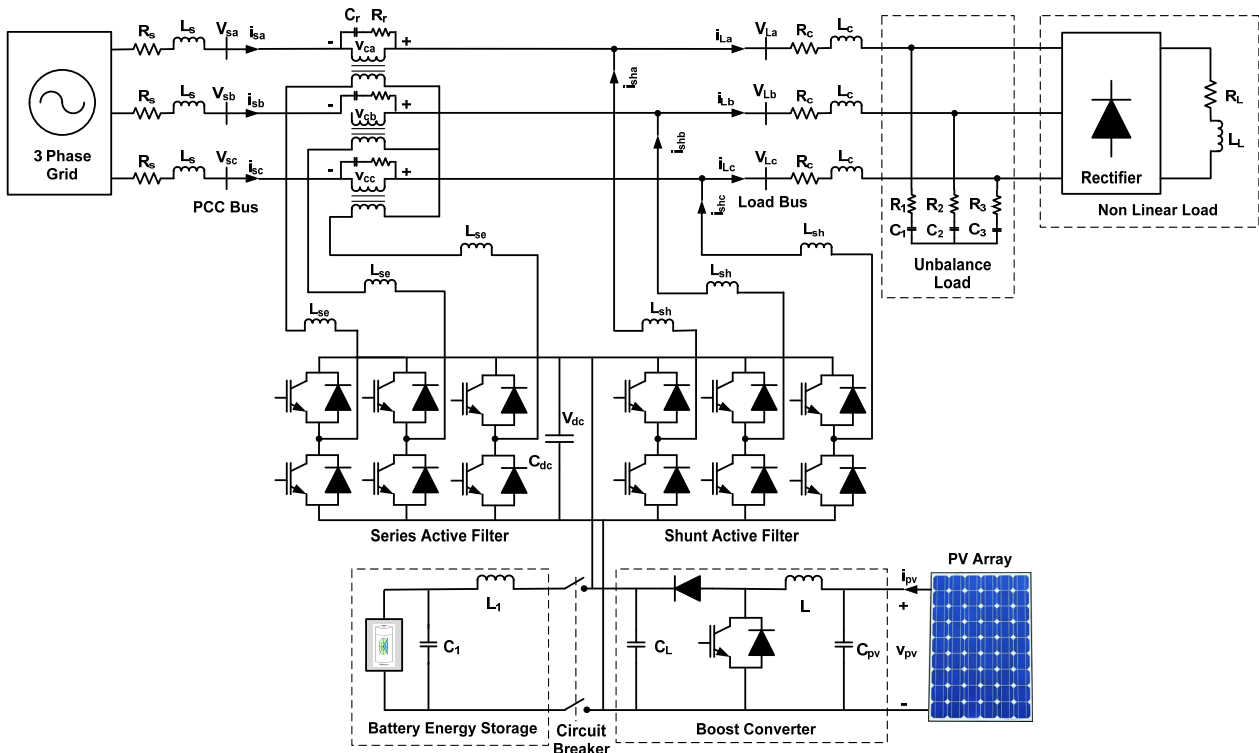


Fig. 1. Proposed model of UPQC supplied by PV and BES

The simulation parameters of the proposed model are showed in Table I. Power quality analysis is performed on PV connected to 3P3W system through UPQC DC link circuit (on-grid), under two conditions i.e. with and without BES. A single phase circuit breaker is used to connect and disconnect PV with BES. Each condition consists of six disturbance scenarios: NL, Unba-NL, Dis-NL, Sag-NL, Swell-NL, and Inter-NL. FLC is used as DC voltage controls in shunt active filter to improve the power quality of the load voltage and source current and they are compared to PI controller. Each scenario uses UPQC controller with PI controller and FLC so there are 12 disturbances in total. The parameters include: voltage and current on source or PCC bus, voltage and current on load bus, voltage harmonics and current harmonics on source bus and voltage harmonics and current harmonics on load bus. The next step is to compare the two controller performances on UPQC to enhance power quality of load voltage and source current under six disturbance conditions.

TABLE I  
SIMULATION PARAMETERS

Devices	Parameters	Design Values
Three Phase Grid	RMS Voltage (LL)	380 Volt
	Frequency	50 Hz
	Line Impedance	$R_s = 0.1$ Ohm $L_s = 15$ mH
Series Active Filter	Series Inductance	$L_{se} = 0.015$ mH
Shunt Active Filter	Shunt Inductance	$L_{sh} = 15$ mH
Injection Transformers	Rating kVA	10 kVA
	Frequency	50 Hz
	Turn Ratio ( $N_1/N_2$ )	1 : 1
Non Linear load	Resistance	$R_L = 60$ Ohm
	Inductance	$L_L = 0.15$ mH
	Load Impedance	$R_c = 0.4$ Ohm
		$L_c = 15$ mH
Unbalance Load	Resistance	$R_1 = 24$ Ohm
		$R_2 = 12$ Ohm
		$R_3 = 6$ Ohm
		$C_1, C_2, C_3 = 2200$ $\mu$ F
DC Link	Capacitance	$C_{DC} = 3000$ $\mu$ F
	DC Voltage	$V_{DC} = 650$ Volt
	Capacitance	$C_{DC} = 3000$ $\mu$ F
Battery Energy Storage	Type	Nickel Metal Hibrid
	DC Voltage	650 V
	Rated Capacity	200 Ah
	Initial SOC	100%
	Inductance	$L_1 = 6$ mH
	Capacitance	$C_1 = 200$ $\mu$ F
PV Generator	Active Power	0.6 kW
	Temperature	25 <sup>o</sup> C
	Irradiance	1000 W/m <sup>2</sup>
PI Parameters	$K_p$ Gain Constant	0.2
	$K_i$ Gain Constant	1.5
Fuzzy model	Method	Mamdani
	Composition	Max-Min
Input membership function	Error ( $V_{dc}$ )	trapmf, trimf
	Delta Error ( $\Delta V_{dc}$ )	trapmf, trimf
Output membership function	Power Loss ( $\bar{p}_{loss}$ )	trapmf, trimf

## II.2. Photovoltaic Model

Fig. 2 shows the equivalent circuit of a solar panel. A solar panel is composed by several PV cells that have series, parallel, or series-parallel external connections [11].

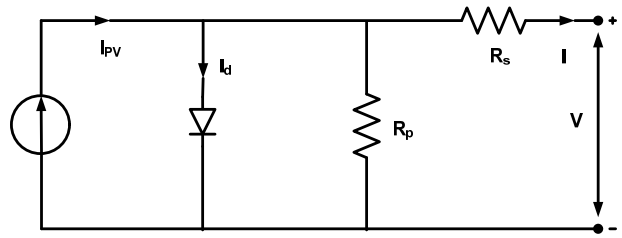


Fig. 2. Equivalent circuit of solar panel

Eq. (1) shows V-I characteristic of a solar panel [11]:

$$I = I_{PV} - I_o \left[ \exp\left(\frac{V + R_s I}{aV_t}\right) - 1 \right] - \frac{V + R_s I}{R_p} \quad (1)$$

where  $I_{PV}$  is the photovoltaic current,  $I_o$  is saturated reverse current, 'a' is the ideal diode constant,  $V_t = N_s K T q^{-1}$  is the thermal voltage,  $N_s$  is the number of series cells,  $q$  is the electron charge,  $K$  is the Boltzmann constant,  $T$  is the temperature of p-n junction,  $R_s$  and  $R_p$  are series and parallel equivalent resistance of the solar panels.

$I_{PV}$  has a linear relation with light intensity and also varies with temperature variations.  $I_o$  is dependent on temperature variations. The values of  $I_{pv}$  and  $I_o$  are calculated as:

$$I_{PV} = (I_{PV,n} + K_1 \Delta T) \frac{G}{G_n} \quad (2)$$

$$I_o = \frac{I_{SC,n} + K_I \Delta T}{\exp(V_{OC,n} + K_V \Delta T) / aV_t - 1} \quad (3)$$

in which  $I_{PV,n}$ ,  $I_{SC,n}$  and  $V_{OC,n}$  are photovoltaic current, short circuit current and open circuit voltage in standard conditions ( $T_n = 25$  C and  $G_n = 1000$  Wm<sup>-2</sup>) respectively.

$K_I$  is the coefficient of short circuit current to temperature,  $\Delta T = T - T_n$  is the temperature deviation from standard temperature,  $G$  is the light intensity and  $K_V$  is the ratio coefficient of open circuit voltage to temperature.

Open circuit voltage, short circuit current and voltage-current corresponding to the maximum power are three important points of I-V characteristic of solar panel.

These points are changed by the variations of atmospheric conditions.

By using Eqs. (4) and (5), which are derived from PV model equations, short circuit current and open circuit voltage can be calculated in different atmospheric conditions:

$$I_{SC} = (I_{SC} + K_1 \Delta T) \frac{G}{G_n} \quad (4)$$

$$V_{OC} = V_{OC} + K_V \Delta T \quad (5)$$

### II.3. Control of Series Active Filter

The main function of series active filter is the sensitive load protection against a number of interference at PCC bus voltage. The control strategy algorithm of the source and load voltage harmonics in series active filter circuit is shown in Fig. 3.

It extracts the unit vector templates from the distorted input supply Furthermore, the templates are expected to be ideal sinusoidal signal with unity amplitude. The distorted supply voltages are measured and divided by the peak amplitude of fundamental input voltage  $V_m$  given by Eq. (6) [6]:

$$V_m = \sqrt{\frac{2}{3}(V_{sa}^2 + V_{sb}^2 + V_{sc}^2)} \quad (6)$$

A three phase locked loop (PLL) is used in order to generate sinusoidal unit vector templates with a phase lagging by the use of sinus function. The reference load voltage signal is determined by multiplying the unit vector templates with the peak amplitude of the fundamental input voltage  $V_m$ . The load reference voltage ( $V_{La}^*$ ,  $V_{Lb}^*$ ,  $V_{Lc}^*$ ) is then compared to the sensed load voltage ( $V_{La}$ ,  $V_{Lb}$ ,  $V_{Lc}$ ) by a pulse width modulation (PWM) controller used to generate the desired trigger signal on the series active filter.

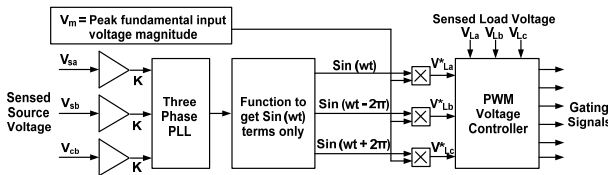


Fig. 3. Control strategy of series active filter

### II.4. Control of Shunt Active Filter

The main function of shunt active filter is the mitigation of power quality problems on the load side.

The control methodology in shunt active filter is that the absorbed current from the PCC bus is a balanced positive sequence current including unbalanced sag voltage conditions in the PCC bus or unbalanced conditions or non-linear loads. In order to obtain satisfactory compensation ceased by disturbance due to non-linear load, many algorithms have been used in literature.

This research used the instantaneous reactive power theory method "p-q theory". The voltages and the currents in Cartesian  $abc$  coordinates can be transformed to Cartesian  $\alpha\beta$  coordinates as expressed in Eqs. (7) and (8) [6]:

$$\begin{bmatrix} v_\alpha \\ v_\beta \end{bmatrix} = \begin{bmatrix} 1 & -1/2 & -1/2 \\ 1 & \sqrt{3}/2 & -\sqrt{3}/2 \end{bmatrix} \begin{bmatrix} V_a \\ V_b \\ V_c \end{bmatrix} \quad (7)$$

$$\begin{bmatrix} i_\alpha \\ i_\beta \end{bmatrix} = \begin{bmatrix} 1 & -1/2 & -1/2 \\ 1 & \sqrt{3}/2 & -\sqrt{3}/2 \end{bmatrix} \begin{bmatrix} i_{La} \\ i_{Lb} \\ i_{Lc} \end{bmatrix} \quad (8)$$

Eq. (9) shows the computation of real power ( $p$ ) and imaginary power ( $q$ ). Real and imaginary powers are measured instantaneously in matrix and their form is given.

Eq. (10) shows the presence of oscillating and average components in instantaneous power [13]:

$$\begin{bmatrix} p \\ q \end{bmatrix} = \begin{bmatrix} v_\alpha & v_\beta \\ -v_\beta & v_\alpha \end{bmatrix} \begin{bmatrix} i_\alpha \\ i_\beta \end{bmatrix} \quad (9)$$

$$p = \bar{p} + \tilde{p} \quad ; \quad q = \bar{q} + \tilde{q} \quad (10)$$

where  $\bar{p}$  is the direct component of real power,  $\tilde{p}$  is the fluctuating component of real power,  $\bar{q}$  is the direct component of imaginary power,  $\tilde{q}$  is the fluctuating component of imaginary power. The total imaginary power ( $q$ ) and the fluctuating component of real power are selected as power references and current references and they are utilized through the use of Eq. (11) to compensate harmonic and reactive power [14]:

$$\begin{bmatrix} i_{c\alpha}^* \\ i_{c\beta}^* \end{bmatrix} = \frac{1}{v_\alpha^2 + v_\beta^2} \begin{bmatrix} v_\alpha & v_\beta \\ v_\beta & -v_\alpha \end{bmatrix} \begin{bmatrix} -\tilde{p} + \bar{p}_{loss} \\ -q \end{bmatrix} \quad (11)$$

The signal  $\bar{p}_{loss}$  is obtained from voltage regulator and it is utilized as average real power. It can also be specified as the instantaneous active power which corresponds to the resistive loss and the switching loss of the UPQC.

The error obtained on comparing the actual DC-link capacitor voltage with the reference value is processed in FLC, engaged by voltage control loop as it minimizes the steady state error of the voltage across the DC link to zero. The compensating currents ( $i_{c\alpha}^*$ ,  $i_{c\beta}^*$ ) required to meet the power demand of load are shown in Eq. (11).

These currents are represented in  $\alpha$ - $\beta$  coordinates. Eq. (12) is used to acquire the phase current required for compensation.

These source phase currents ( $i_{sa}^*$ ,  $i_{sb}^*$ ,  $i_{sc}^*$ ) are represented in a-b-c axis obtained from compensating current in the  $\alpha$ - $\beta$  coordinates in Eq. (12) [14]:

$$\begin{bmatrix} i_{sa}^* \\ i_{sb}^* \\ i_{sc}^* \end{bmatrix} = \sqrt{\frac{2}{3}} \begin{bmatrix} 1 & 0 \\ -1/2 & \sqrt{3}/2 \\ -1/2 & -\sqrt{3}/2 \end{bmatrix} \begin{bmatrix} i_{c\alpha}^* \\ i_{c\beta}^* \end{bmatrix} \quad (12)$$

Fig. 4 shows a control of shunt active filter.

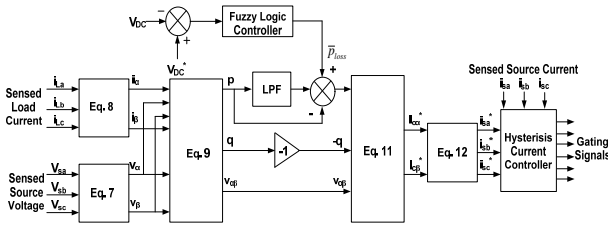


Fig. 4. Control strategy of shunt active filter

The proposed model of UPQC supplied by PV and BES has been shown in Fig. 1. From the figure it can be seen that the PV and BES are connected to the DC link through a DC-DC boost converter circuit. The PV generator partially distributes power to the load and the remaining is transferred to the three phase grid. The load consists of non linear and unbalanced load. The non-linear load is a diode rectifier circuit with the RL load type, while the unbalanced load is a three phase RC load with different  $R$  value on each phase. In order to be economically efficient, PV generator must always work in maximum power point (MPP) condition. In this research, the MPPT method used is P and O algorithm.

In order to operate properly, the UPQC device must have a minimum DC link voltage ( $V_{dc}$ ). The value of common DC link voltage depends on the instantaneous energy available to the UPQC is defined by Eq. (13) [12]:

$$V_{dc} = \frac{2\sqrt{2}V_{LL}}{\sqrt{3}m} \quad (13)$$

where  $m$  is the modulation index and  $V_{LL}$  is the AC grid line voltage of UPQC. Considering modulation index as 1 and for line to line grid voltage ( $V_{LL} = 380$  volt), the  $V_{dc}$  is obtained 620,54 volt and is selected as 650 volt.

The input of shunt active filter showed in Fig. 5 is DC voltage ( $V_{dc}$ ) and reference DC voltage ( $V_{dc}^*$ ), while the output is  $\bar{p}_{loss}$  by using PI controller. Then, the  $\bar{p}_{loss}$  is a variable input to generate the reference source current ( $I_{sa}^*$ ,  $I_{sb}^*$ , and  $I_{sc}^*$ ). The reference source current output is then compared to sensed source current ( $I_{sa}$ ,  $I_{sb}$ , and  $I_{sc}$ ) by the current hysteresis control to generate trigger signal in IGBT circuit of shunt active filter. In this research, FLC as DC voltage control algorithm on shunt active filter is proposed and compared with PI controller. The FLC is capable to reduce oscillation and generate quick convergence calculation during disturbances. This method is also used to overcome the weakness of PI control in determining proportional gain ( $K_p$ ) and integral gain constant ( $K_i$ ) which still use trial and error method.

### II.5. Fuzzy Logic Controller

The research begins by determining  $\bar{p}_{loss}$  as the input variable to result the reference source current on current hysteresis controller to generate a trigger signal on the IGBT shunt active filter of UPQC using PI controller ( $K_p$

= 0.2 and  $K_i = 1.5$ ). By using the same procedure,  $\bar{p}_{loss}$  is also determined by using FLC. The FLC has been widely used in recent industrial processes because it has heuristic, simpler, more effective and has multi rule based variables in both linear and non-linear system variations. The main components of FLC are fuzzification, decision making (rulebase, database, reason mechanism) and defuzzification, showed in Fig. 5.

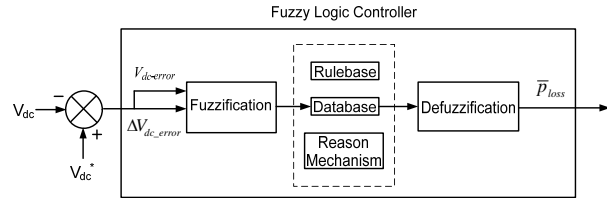


Fig. 5. Diagram block of FLC

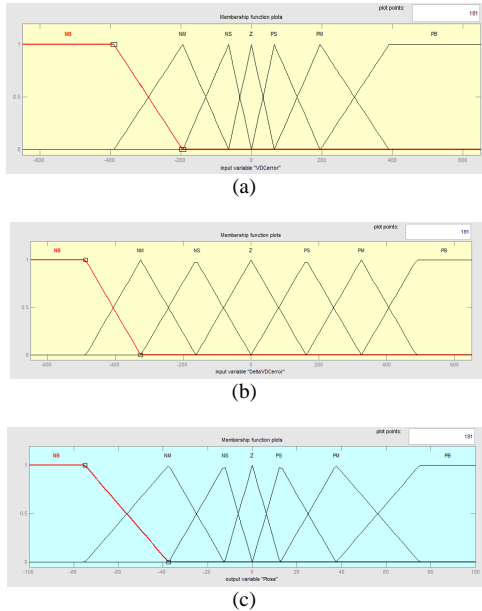
The fuzzy rule algorithm collects a number of fuzzy control rules in a particular order. This rule is used to control the system to meet the desired performance requirements and they are designed from a number of intelligent system control knowledge. The fuzzy inference of FLC uses Mamdani method related to max-min composition. The fuzzy inference system in FLC consists of three parts: rule base, database, and reasoning mechanism. Rule base consists of a number of If-Then rules for the proper operation of the controller. The If part of the rule is called antecedent and the Then section is called consequence. A number of these rules can be considered as similar responses made by human thought processes and controllers using linguistic input variables, gaining after fuzzification for operation of those rules.

The database consists of all user defined membership functions that will be used in a number of these rules.

Reasoning mechanisms basically process the rules provided based on certain rules and given conditions that provide the required results to user [15].

The FLC method is performed by determining the input variables  $V_{dc}$  ( $V_{dc-error}$ ) and delta  $V_{dc}$  ( $\Delta V_{dc-error}$ ), seven linguistic fuzzy sets, the operation fuzzy block system (fuzzification, fuzzy rule base and defuzzification),  $V_{dc-error}$  and  $\Delta V_{dc-error}$  during fuzzification process, the fuzzy rule base table, the crisp value to determine  $\bar{p}_{loss}$  in defuzzification phase. The  $\bar{p}_{loss}$  is one a variable input to obtain compensating currents ( $i_{ca}^*$ ,  $i_{cb}^*$ ) in Eq. (11). During fuzzification process, a number of input variables are calculated and converted into linguistic variables based on a subset called membership function. The  $V_{dc}$  error ( $V_{dc-error}$ ) and the delta  $V_{dc}$  ( $\Delta V_{dc-error}$ ) error are the proposed input variable system and the output variable is  $\bar{p}_{loss}$ . In order translate these variables, each input and output variable is designed using seven membership functions: Negative Big (NB), Negative Medium (NM), Negative Small (NS), Zero (Z), Positive Small (PS), Positive Medium (PM) and Positive Big (PB).

The membership functions of crisp input and output are presented with triangle and trapezoid membership functions. The value of  $V_{dc-error}$  ranges from -650 to 650,  $\Delta V_{dc-error}$  from -650 to 650, and  $\bar{p}_{loss}$  from -100 to 100. The input and output MFs are shown in Figs. 6.



Figs. 6. MFs (a)  $V_{dc-error}$ , (b)  $\Delta V_{dc-error}$ , (c) and  $\bar{p}_{loss}$

After the  $V_{dc-error}$  and the  $\Delta V_{dc-error}$  are obtained, two input membership functions are converted to linguistic variables and they are used as input functions for FLC.

The output membership function is generated using inference blocks and the basic rules of FLC as shown in Table II.

TABLE II  
FUZZY RULE BASE

$V_{dc-error}$	NM	NB	NS	Z	PS	PB	PM
$\Delta V_{dc-error}$	PM	Z	PS	PS	PM	PM	PB
PB	NS	Z	PS	PS	PM	PM	PB
PS	NS	NS	Z	PS	PS	PM	PM
Z	NM	NS	NS	Z	PS	PS	PM
NS	NM	NM	NS	NS	Z	PS	PS
NB	NB	NM	NM	NS	NS	Z	PS
NM	NB	NB	NM	NM	NS	NS	Z

Finally the defuzzification block operates to convert generated  $\bar{p}_{loss}$  output from linguistic to numerical variable again. Then it becomes an input variable for current hysteresis controller to produce trigger signal on the IGBT circuit of UPQC shunt active filter to reduce source current and load voltage harmonics, while simultaneously improving power quality of 3P3W system under six interference scenarios due to integration of PV and BES into DC link circuit of UPQC.

### III. Result and Discussion

The analysis of the proposed model is investigated

through the determination of six disturbance scenarios i.e. NL, Unba-NL, Dis-NL, Sag-NL, Swell-NL, and Inter-NL.

In Scenario 1, the system is connected to a non-linear load with  $R_L$  and  $L_L$  of 60 Ohm and 0.15 mH respectively.

In Scenario 2, the system is connected to anon-linear load and during 0.3 s since  $t = 0.2$  s to  $t = 0.5$  s connected to unbalance three phase load with  $R_1, R_2, R_3$  as 6 Ohm, 12 Ohm, 24 Ohm respectively, and value of  $C_1, C_2, C_3$  as 2200  $\mu$ F.

In Scenario 3, the system is connected to a non-linear load and source voltage generating 5<sup>th</sup> and 7<sup>th</sup> harmonic components with individual harmonic distortion values of 5% and 2% respectively.

In Scenario 4, the system is connected to a non-linear load and source experiences a sag voltage disturbance of 50% for 0.3 s between  $t = 0.2$  s to  $t = 0.5$  s.

In Scenario 5, the system is connected to a non-linear load and source experiences a swell voltage disturbance of 50% for 0.3 s between  $t = 0.2$  s to  $t = 0.5$  s.

In Scenario 6, the system is connected to a non-linear load and source experiences an interruption voltage interference of 100% for 0.3 s between  $t = 0.2$  s to  $t = 0.5$  s. Each scenario uses UPQC control with PI control and FLC so the total number of disturbances is 12 scenarios.

Then, by using Matlab/Simulink, the system is executed according to the desired scenario to obtain the curve of source voltage ( $V_s$ ), load voltage ( $V_L$ ), compensation voltage ( $V_C$ ), source current ( $I_s$ ), load current ( $I_L$ ), and DC link voltage ( $V_{dc}$ ).

Then, THD value of source voltage, source current, load voltage, and load current in each phase as well as average THD value (Avg THD) are obtained based on the curves. THD in each phase is determined in one cycle started at  $t = 0.35$  s.

The average results of source voltage, source current, load voltage, and load current on proposed systes of PV connected to DC link circuit without and with BES are presented in Tables III and IV. Futhermore, THD in each phase and average THD of proposed system are showed in Tables V and VI.

Table III shows that UPQC supplied by PV without BES in 3P3W system with PI and FLC control for interference scenarios 1 to 5, is able to maintain average load voltages above 310 volt.

The difference is that in Scenario 6 (Inter-NL), PI control generates load voltage of 240.4 volt and if using FLC drops to 215 volt.

Reviewed from source current using PI control, the highest and the lowest average source currents are generated by interference Scenarios 2 (Unba-NL) and 4 (Swell-NL) of 29.84 A and 8,462 A respectively.

Otherwise if using FLC the highest and the lowest average source current drop on same both disturbance scenarios of 29.78 A and 8.363 A respectively.

Table IV indicates that UPQC supplied by PV using BES in 3P3W system with PI and FLC controls for scenarios 1 to 5 is able to produce average load voltage



above 307 V.

While in Scenario 6 (Inter-NL), FLC produces a higher average load voltage of 304.1 V than when using PI control of 286.7 volt PI.

Reviewed from average source current with PI control, the highest and lowest average source current are generated by interference Scenarios 2 (Unba-NL) and 4 (Sag-NL) of 28.15 A and 7,246 A respectively. While if using FLC, the highest and lowest average source current are achieved in Scenario 2 (Unba-NL) and Scenario 5 (Swell-NL) of 28.84 A and 8,392 A.

Table V shows that the average THD of  $V_L$  of UPQC supplied by PV without BES in 3P3W for interference Scenarios 1 to 5 using PI control is within the limits prescribed in IEEE 519. In this condition PI controller is also capable to maintain and to improve the average THD of load voltage within the limits of IEEE 519.

The highest and the lowest average THD load voltages are achieved under scenario interruption conditions 6 (Inter-NL) and Scenario 2 (Unba-NL): 15.69% and 0.74% respectively. PI controller is also able to reduce average THD source voltage in Scenario 6 (Inter-NL) by 93.97% to 15.69% on the load side.

The highest and the lowest average THD of source current are achieved in scenario 6 (Inter-NL) and Scenario 2 (Unba-NL): 17.07% and 4.44% respectively.

Table V also shows that average THD of load voltage of UPQC system supplied by PV without BES using FLC

in disturbance Scenarios 1 to 5, has fulfilled the limits prescribed in IEEE 519. FLC method is also capable to maintain and to improve average THD of load voltage within the IEEE 519 limit.

The highest and lowest average THD of  $V_L$  are achieved under Scenario 6 (Inter-NL) and Scenario 4 (Sag-NL) of 35.51% and 0.52. The implementation of FLC method is also able to reduce average THD of  $V_S$  in Scenario 6 (Inter-NL) by 90.56% to 35.51% on load side.

The highest and the lowest average THD of  $I_S$  are achieved in Scenario 6 (Inter-NL) and Scenario 2 (Unba-NL) of 36.20% and 4.65%. UPQC system supplied by PV without BES in six interference scenarios using PI control and FLC is able to improve average THD of  $I_S$  better on average THD of  $I_L$ .

Table VI shows that average THD of  $V_L$  from UPQC supplied by PV with BES in 3P3W system for interference Scenarios 1 to 5 using PI control is within the limits prescribed in IEEE 519. In this condition PI controller is also capable to maintain average THD of  $V_L$  within the limits of IEEE 519.

The highest and the lowest average THD of  $V_L$  are achieved under Scenario 6 (Inter-NL) and Scenario 2 (Unba-NL): 25.25% and 2.34% respectively. PI controller is also able to mitigate average THD of  $V_S$  in Scenario 6 (Inter-NL) from not accessed (NA) to 25.25% on the load side.

TABLE III  
VOLTAGE AND CURRENT OF 3P3W SYSTEM USING UPQC SUPPLIED BY PV WITHOUT BES

Scenarios	Source Voltage $V_S$ (Volt)				Load Voltage $V_L$ (Volt)				Source Current $I_S$ (Ampere)				Load Current $I_L$ (Ampere)			
	Ph A	Ph B	Ph C	Avg	Ph A	Ph B	Ph C	Avg	Ph A	Ph B	Ph C	Avg	Ph A	Ph B	Ph C	Avg
PI Controller																
1. NL	309.5	309.5	309.5	<b>309.5</b>	310.0	310.0	310.0	<b>310.0</b>	8.828	8.838	8.858	<b>8.841</b>	8.586	8.586	8.585	<b>8.586</b>
2. Unba-NL	307.8	307.8	307.8	<b>307.8</b>	310.2	310.2	310.3	<b>310.2</b>	32.15	26.66	30.71	<b>29.84</b>	22.65	34.26	34.70	<b>30.54</b>
3. Dist-NL	309.5	309.5	309.5	<b>309.5</b>	308.5	312.1	310.5	<b>310.5</b>	8.936	8.863	10.73	<b>9.510</b>	8.522	8.757	8.601	<b>8.627</b>
4. Sag-NL	153.8	153.8	153.8	<b>153.8</b>	310.1	310.1	310.1	<b>310.1</b>	13.39	13.33	13.41	<b>13.38</b>	8.589	8.589	8.588	<b>8.589</b>
5. Swell-NL	464.4	464.4	464.4	<b>464.4</b>	310.1	310.1	310.1	<b>310.1</b>	8.457	8.468	8.460	<b>8.462</b>	8.558	8.590	8.558	<b>8.587</b>
6. Inter-NL	1.190	1.316	1.237	<b>1.247</b>	229.2	249.1	242.8	<b>240.4</b>	11.31	11.86	11.91	<b>35.08</b>	6.443	6.698	6.289	<b>6.477</b>
Fuzzy Logic Controller																
1. NL	309.5	309.5	309.5	<b>309.5</b>	310.1	310.1	310.0	<b>310.1</b>	8.769	8.738	8.811	<b>8.773</b>	8.578	8.588	8.587	<b>8.584</b>
2. Unba-NL	307.3	307.8	307.8	<b>307.8</b>	310.2	310.3	310.2	<b>310.2</b>	32.01	26.66	30.65	<b>29.78</b>	22.65	34.65	34.69	<b>30.66</b>
3. Dist-NL	309.4	309.5	309.5	<b>309.5</b>	309.6	312.1	309.9	<b>310.5</b>	8.938	8.820	8.916	<b>8.891</b>	8.552	8.766	8.586	<b>8.635</b>
4. Sag-NL	153.8	153.8	153.8	<b>153.8</b>	310.1	310.0	310.1	<b>310.1</b>	13.52	13.46	13.56	<b>13.51</b>	8.558	8.587	8.589	<b>8.578</b>
5. Swell-NL	464.4	464.7	464.7	<b>464.7</b>	310.1	310.1	310.1	<b>310.1</b>	8.353	8.371	8.365	<b>8.363</b>	8.591	8.588	8.587	<b>8.589</b>
6. Inter-NL	1.259	1.285	1.530	<b>1.358</b>	209.9	193.7	242.7	<b>215.4</b>	13.28	11.49	14.07	<b>12.95</b>	6.459	5.003	6.299	<b>5.921</b>

TABLE IV  
VOLTAGE AND CURRENT OF 3P3W SYSTEM USING UPQC SUPPLIED BY PV WITH BES

Scenarios	Source Voltage $V_S$ (Volt)				Load Voltage $V_L$ (Volt)				Source Current $I_S$ (Ampere)				Load Current $I_L$ (Ampere)			
	Ph A	Ph B	Ph C	Avg	Ph A	Ph B	Ph C	Avg	Ph A	Ph B	Ph C	Avg	Ph A	Ph B	Ph C	Avg
PI Controller																
1. NL	309.6	309.6	309.6	<b>309.6</b>	307.6	307.8	307.7	<b>307.7</b>	7.766	7.793	7.759	<b>7.773</b>	8.528	8.529	8.533	<b>8.530</b>
2. Unba-NL	307.4	308.0	308.0	<b>307.8</b>	308.3	308.7	308.3	<b>308.4</b>	31.00	24.84	28.73	<b>28.15</b>	22.50	34.12	34.52	<b>30.38</b>
3. Dist-NL	309.6	309.6	309.6	<b>309.6</b>	313.8	314.3	317.4	<b>317.4</b>	7.897	7.919	7.867	<b>7.895</b>	8.748	8.704	8.785	<b>8.746</b>
4. Sag-NL	154.5	154.5	154.5	<b>154.5</b>	307.1	307.3	307.3	<b>307.2</b>	7.235	7.276	7.226	<b>7.246</b>	8.509	8.514	8.510	<b>8.511</b>
5. Swell-NL	464.7	464.7	464.7	<b>464.7</b>	308.6	308.7	308.6	<b>308.6</b>	7.979	7.980	7.964	<b>7.975</b>	8.550	8.553	8.554	<b>8.553</b>
6. Inter-NL	0.5359	1.385	0.8501	<b>0.9238</b>	310.2	259.8	290.2	<b>286.7</b>	7.392	12.67	6.045	<b>8.703</b>	8.707	7.747	7.637	<b>8.031</b>
Fuzzy Logic Controller																
1. NL	309.5	309.5	309.5	<b>309.5</b>	307.7	307.9	307.7	<b>307.8</b>	8.420	8.426	8.416	<b>8.421</b>	8.527	8.532	8.531	<b>8.530</b>
2. Unba-NL	307.4	307.9	308.0	<b>307.8</b>	308.5	308.7	308.4	<b>308.5</b>	31.66	25.50	29.36	<b>28.84</b>	22.52	34.11	35.52	<b>30.72</b>
3. Dist-NL	309.6	309.5	309.5	<b>309.5</b>	313.4	312.9	315.9	<b>314.1</b>	8.516	8.565	8.496	<b>8.526</b>	8.741	8.677	8.736	<b>8.718</b>
4. Sag-NL	154.4	154.4	154.4	<b>154.4</b>	307.3	307.3	307.2	<b>307.3</b>	8.563	8.560	8.561	<b>8.561</b>	8.514	8.517	8.512	<b>8.515</b>
5. Swell-NL	464.6	464.6	464.6	<b>464.6</b>	308.6	308.8	308.6	<b>308.7</b>	8.396	8.389	8.389	<b>8.392</b>	8.552	8.556	8.554	<b>8.554</b>
6. Inter-NL	0.4467	0.3918	0.3801	<b>0.4062</b>	314.0	293.4	304.9	<b>304.1</b>	4.024	3.778	3.608	<b>3.804</b>	8.874	8.195	8.193	<b>8.421</b>



TABLE V  
HARMONICS OF 3P3W SYSTEM USING UPQC SUPPLIED BY PV WITHOUT BES

Scenarios	Source Voltage THD (%)				Load Voltage THD (%)				Source Current THD (%)				Load Current THD (%)			
	Ph A	Ph B	Ph C	Avg	Ph A	Ph B	Ph C	Avg	Ph A	Ph B	Ph C	Avg	Ph A	Ph B	Ph C	Avg
PI Controller																
1. NL	0.79	0.79	0.79	<b>0.79</b>	0.83	0.83	0.82	<b>0.83</b>	11.07	10.79	10.95	<b>10.94</b>	22.31	22.31	22.32	<b>22.31</b>
2. Unba-NL	0.68	0.70	0.67	<b>0.69</b>	0.74	0.77	0.71	<b>0.74</b>	4.520	4.540	4.240	<b>4.44</b>	5.280	2.050	2.700	<b>3.34</b>
3. Dist-NL	5.41	5.44	5.52	<b>5.46</b>	4.18	9.93	3.93	<b>6.02</b>	10.61	10.91	10.73	<b>10.75</b>	22.70	20.86	21.07	<b>21.54</b>
4. Sag-NL	1.03	1.03	1.03	<b>1.03</b>	0.52	0.52	0.52	<b>0.52</b>	11.60	11.57	11.27	<b>11.48</b>	22.29	22.29	22.28	<b>22.49</b>
5. Swell-NL	0.69	0.69	0.70	<b>0.69</b>	1.08	1.09	1.09	<b>1.09</b>	11.38	11.42	11.63	<b>11.48</b>	22.32	22.30	22.32	<b>22.31</b>
6. Inter-NL	98.72	87.77	95.42	<b>93.97</b>	13.58	16.61	16.87	<b>15.69</b>	15.62	16.56	19.01	<b>17.07</b>	18.21	20.16	21.06	<b>19.81</b>
Fuzzy Logic Controller																
1. NL	0.79	0.78	0.77	<b>0.78</b>	0.82	0.82	0.80	<b>0.81</b>	11.73	10.83	11.06	<b>11.21</b>	22.23	22.32	22.32	<b>22.29</b>
2. Unba-NL	0.68	0.70	0.66	<b>0.68</b>	0.71	0.74	0.70	<b>0.72</b>	4.560	4.900	4.470	<b>4.65</b>	5.290	2.050	2.700	<b>3.35</b>
3. Dist-NL	5.41	5.43	5.52	<b>5.45</b>	3.54	10.34	3.92	<b>5.93</b>	10.92	10.51	10.66	<b>10.69</b>	22.78	20.77	21.30	<b>21.62</b>
4. Sag-NL	1.02	1.02	1.03	<b>1.02</b>	0.52	0.52	0.52	<b>0.52</b>	11.99	12.02	11.99	<b>12.00</b>	22.31	22.31	22.29	<b>22.30</b>
5. Swell-NL	0.67	0.69	0.69	<b>0.68</b>	1.06	1.08	1.08	<b>1.07</b>	11.65	11.49	11.79	<b>11.64</b>	22.30	22.32	22.31	<b>22.31</b>
6. Inter-NL	91.76	97.26	82.66	<b>90.56</b>	39.40	24.79	42.32	<b>35.51</b>	41.57	23.11	43.92	<b>36.20</b>	40.18	35.29	42.75	<b>48.98</b>

TABLE VI  
HARMONICS OF 3P3W SYSTEM USING UPQC SUPPLIED BY PV WITH BES

Scenarios	Source Voltage THD (%)				Load Voltage THD (%)				Source Current THD (%)				Load Current THD (%)			
	Ph A	Ph B	Ph C	Avg	Ph A	Ph B	Ph C	Avg	Ph A	Ph B	Ph C	Avg	Ph A	Ph B	Ph C	Avg
PI Controller																
1. NL	2.35	2.36	2.32	<b>2.34</b>	2.48	2.50	2.46	<b>2.48</b>	12.89	12.72	12.92	<b>12.84</b>	22.32	22.34	22.32	<b>22.33</b>
2. Unba-NL	2.29	2.20	2.24	<b>2.24</b>	2.43	2.23	2.37	<b>2.34</b>	2.660	2.330	2.240	<b>2.410</b>	5.230	2.070	2.660	<b>3.320</b>
3. Dist-NL	5.84	5.86	5.94	<b>5.88</b>	6.36	5.90	6.58	<b>6.28</b>	12.75	12.64	13.06	<b>12.82</b>	21.92	22.16	22.33	<b>22.14</b>
4. Sag-NL	4.69	4.75	4.81	<b>4.75</b>	2.46	2.48	2.53	<b>2.49</b>	14.26	13.96	14.16	<b>14.13</b>	22.28	22.31	22.28	<b>22.29</b>
5. Swell-NL	1.56	1.53	1.55	<b>1.55</b>	2.47	2.43	2.45	<b>2.45</b>	12.51	12.36	12.44	<b>12.44</b>	22.34	22.32	22.32	<b>22.33</b>
6. Inter-NL	NA	NA	NA	<b>NA</b>	32.11	15.09	28.54	<b>25.25</b>	270.90	145.89	275.67	<b>230.82</b>	47.70	34.58	36.29	<b>39.53</b>
Fuzzy Logic Controller																
1. NL	2.35	2.33	2.35	<b>2.34</b>	2.48	2.46	2.49	<b>2.47</b>	11.83	11.82	11.84	<b>11.83</b>	22.33	22.32	22.33	<b>22.33</b>
2. Unba-NL	2.25	2.27	2.20	<b>2.24</b>	2.39	2.41	2.34	<b>2.38</b>	2.620	2.400	2.220	<b>2.413</b>	5.230	2.100	2.640	<b>3.323</b>
3. Dist-NL	5.83	5.88	5.93	<b>5.88</b>	6.23	5.93	6.69	<b>6.28</b>	11.83	11.90	12.14	<b>11.96</b>	21.84	22.34	22.53	<b>22.24</b>
4. Sag-NL	4.71	4.76	4.79	<b>4.75</b>	2.46	2.48	2.50	<b>2.48</b>	11.91	11.88	11.86	<b>11.89</b>	22.27	22.32	22.32	<b>22.31</b>
5. Swell-NL	1.55	1.54	1.54	<b>1.54</b>	2.45	2.44	2.46	<b>2.45</b>	11.90	11.84	11.85	<b>11.86</b>	22.36	22.33	22.35	<b>22.35</b>
6. Inter-NL	NA	NA	NA	<b>NA</b>	13.05	6.60	11.15	<b>10.27</b>	30.61	34.72	31.57	<b>32.30</b>	24.25	24.25	24.71	<b>24.40</b>

The highest and the lowest average THD of  $I_S$  are achieved in Scenario 6 (Inter-NL) and Scenario 2 (Unba-NL): 230.82% and 2.41% respectively.

Table VI also indicates that average THD of  $V_L$  of UPQC system supplied by PV with BES using FLC in disturbance Scenarios 1 to 5, has fulfilled limits prescribed in IEEE 519. FLC method is also capable to keep average THD of  $V_L$  within IEEE 519.

The highest and the lowest average THD of  $V_L$  are achieved under Scenario 6 (Inter-NL) and Scenario 2 (Unba-NL): 10.27% and 2.38%.

The use of FLC method is also useful to reduce average THD on  $V_S$  in Scenario 6 (Inter-NL) from NA to 10.27% on load side.

The highest and the lowest average THD of  $I_S$  are achieved in Scenario 6 (Inter-NL) and Scenario 2 (Unba-NL) of 32.30% and 2.413%, respectively. UPQC system supplied by PV with BES in six interference scenarios using PI control and FLC is able to improve average THD of  $I_S$  better on average THD of  $I_L$ .

Figs. 7 and Figs. 8 present UPQC-PV performance using FLC without and with BES in Scenario 4 (Sag-NL) and Scenario 6 (Inter-NL).

Fig. 7(a) shows that in scenario 4 (Sag-NL), UPQC supplied by PV without BES at  $t = 0.2$  s to  $t = 0.5$  s average  $V_S$  drops by 50% from 310.1 V to 153.8 V. In this condition, PV is capable to generate power to the UPQC DC link circuit and injecting  $V_C$  as 153.8 V (Fig.

7(e)) through injection transformer on series active filter so that average  $V_L$  remains stable at 310.1 V (Fig. 7(c)).

During this time, FLC on shunt active filter works to keep  $V_{dc}$  stable and average  $I_S$  increases approach to 13.28 A (Fig. 7(g)) in order to keep average  $I_L$  stable by 8.589 A (Fig. 7(i)).

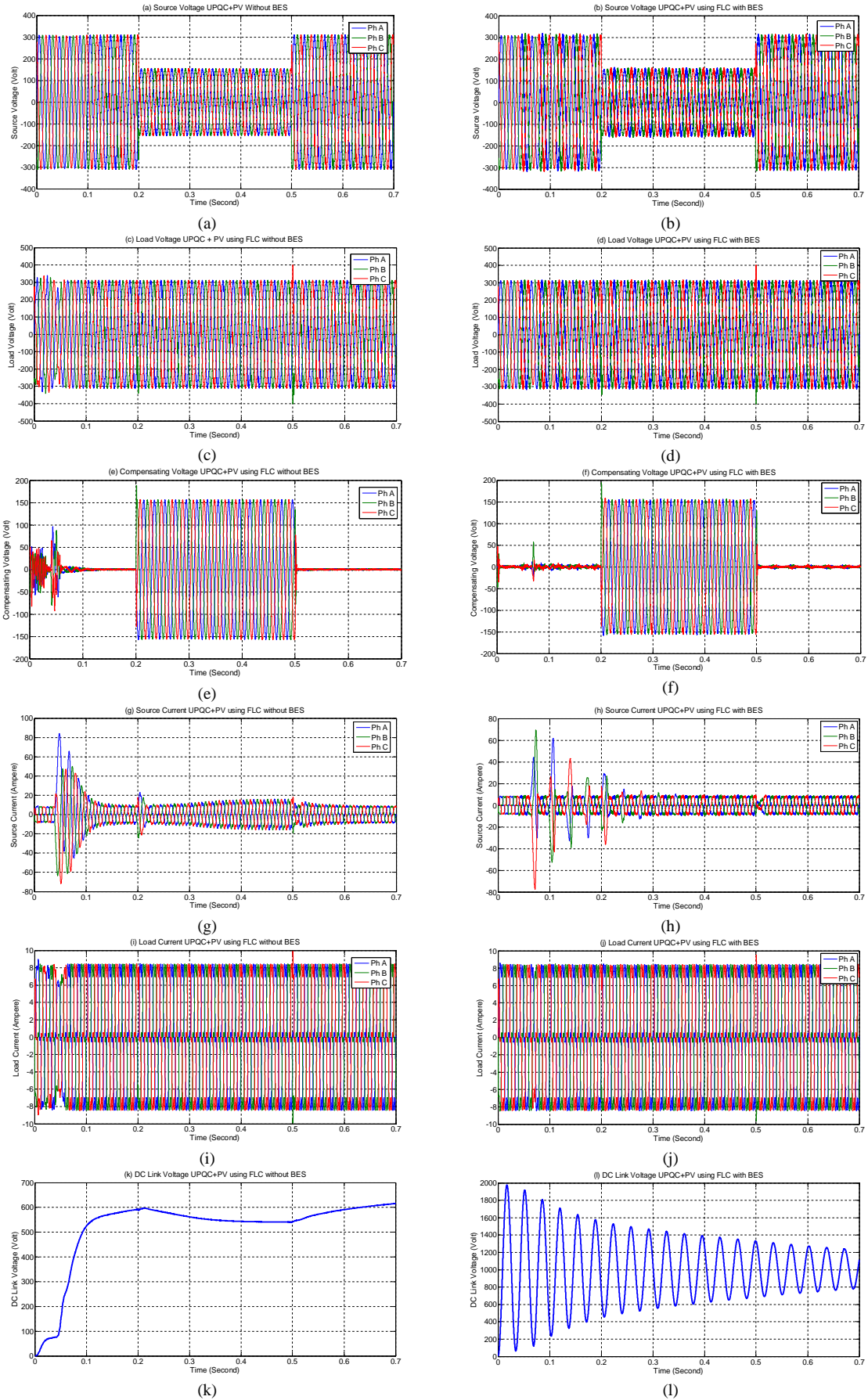
Fig. 8(b) in Scenario 4 (Sag-NL) using BES also shows almost the same performance on average  $V_C$ , average  $V_L$ , and average  $I_L$  presented in Fig. 7(f), Fig. 7(d), and Fig. 7(j) respectively. The difference is that average  $I_S$  is slightly decreased to 8.561 A (Fig. 7(h)).

The addition of BES, besides the fact of being capable to store excess power from PV generator, also serves to inject current into load through DC link (Fig. 7(l)) and shunt active filter to produce average  $I_L$  equal to 8.515 A.

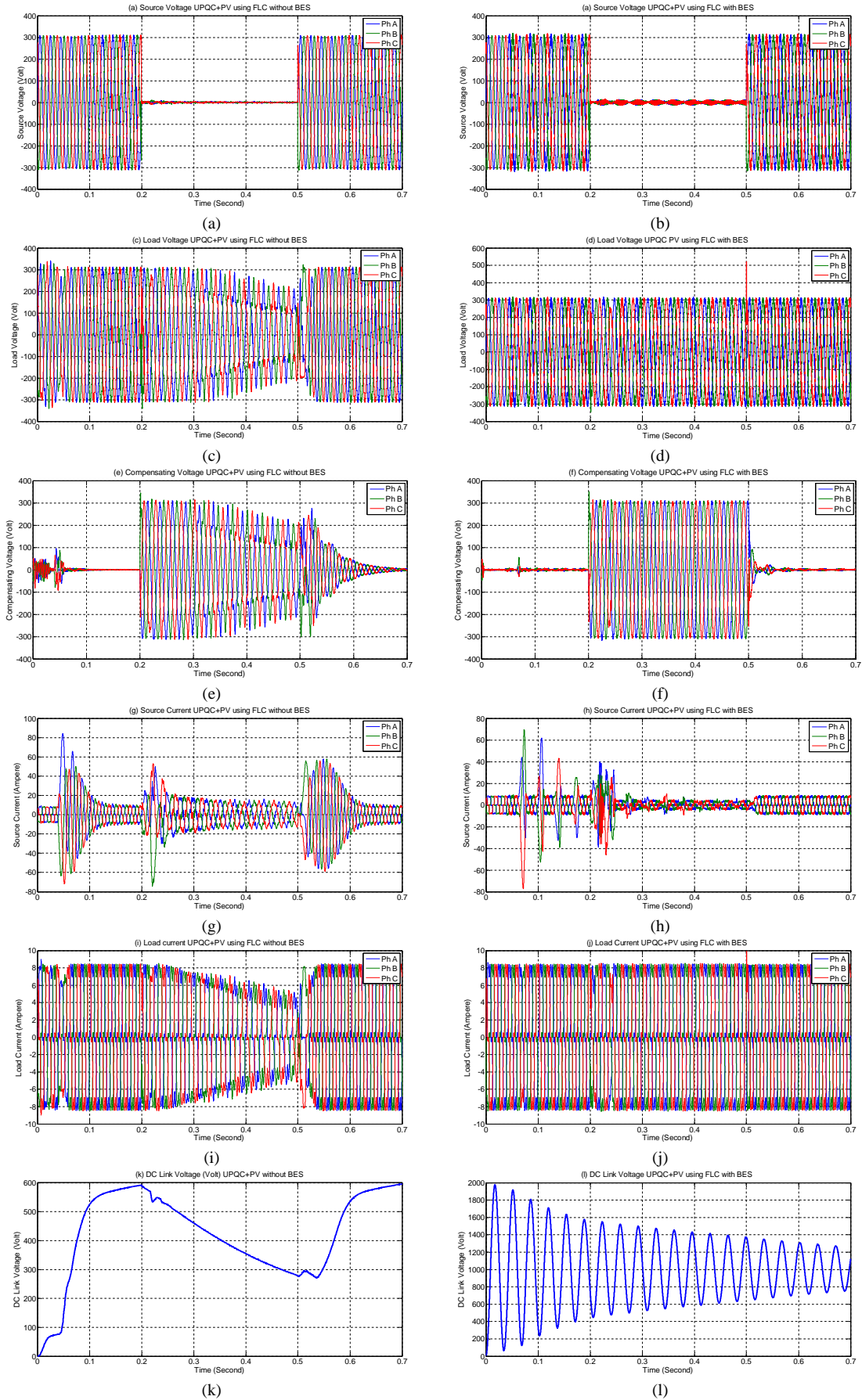
Fig. 8(a) shows that in Scenario 6 (Inter-NL) UPQC supplied PV by without BES at  $t = 0.2$  s to  $t = 0.5$  s, average  $V_S$  falls as 100% to 1.358 V.

In this condition PV is unable to generate the maximum power to UPQC DC link and inject average  $V_C$  in Fig 8(e) through injection transformer on series active filter. So at  $t = 0.2$  s to  $t = 0.5$ , average  $V_L$  in Fig. 8(c) decrease to 215.4 V.

During the disturbance, the implementation of FLC on shunt active filter keeps the maintenance  $V_{dc}$  (Fig 8(k)), interruption voltage causes average  $I_S$  to decrease to 12.29 A (Fig. 8(g)) and average  $I_L$  also decreases to 5.921 A (Fig. 8(i)).

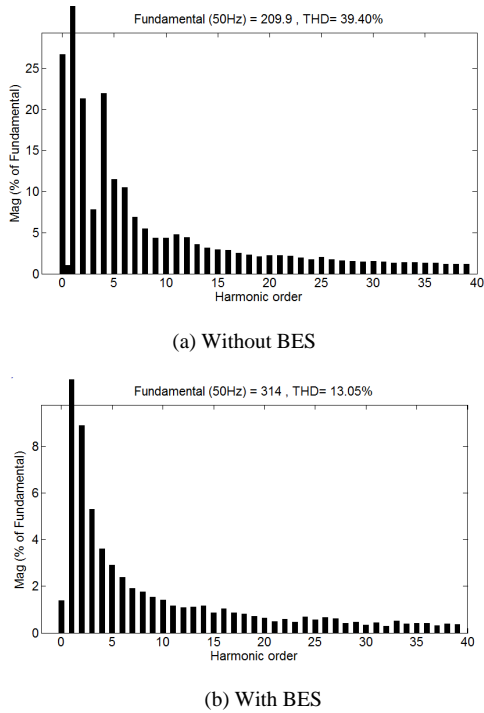


Figs. 7. UPQC supplied PV performance using FLC without and with BES in Scenario 4 (Sag-NL)



Figs. 8. UPQC supplied PV performance using FLC without and with BES in scenario 6 (Inter-NL)

Fig. 8(b) on UPQC supplied by PV with BES at  $t = 0.2$  s to  $t = 0.5$  s average  $V_S$  also drops 100% to 0.4062 V. During the disturbance, PV is able to generate power to UPQC DC link and injecting full average  $V_C$  in Fig. 8(f) through the injection transformer on series active filter so that average  $V_L$  remains stable at 304.1 V (Fig. 8(d)). As long fault period, although nominal of average  $I_S$  drops to 3.804 A, the combination of PV and BES is able to generate power, store excess energy of PV, and inject current into load through shunt active filter so that  $I_L$  in Fig. 8(l) remains as 8.421 A. Figs. 9 show spectra of load voltage harmonics on phase A of UPQC supplied by PV using FLC without and with BES in Scenario 6.



Figs. 9. Spectra of load voltage harmonics on phase A UPQC supplied PV using FLC in Scenario 6 (Inter-NL)

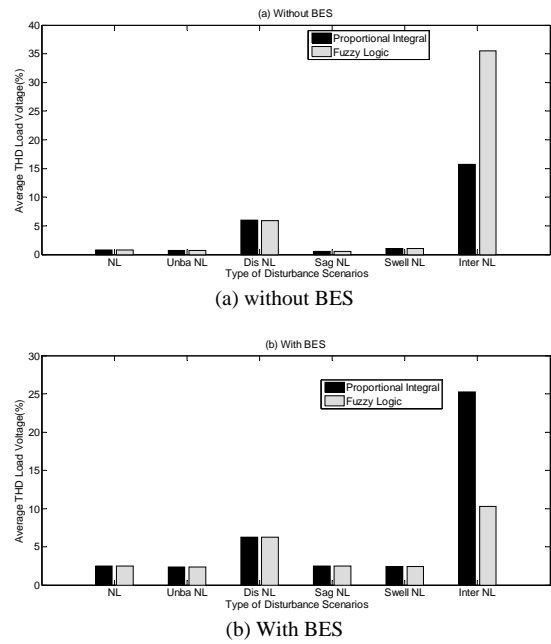
Fig. 10 and Fig. 11 show the performances of average THD of load voltage ( $V_L$ ) and source current ( $I_S$ ) on UPQC supplied by PV using PI controller and FLC without and with BES in six disturbance scenarios.

Fig. 10(a) shows that in Scenario 1(NL), Scenario 2 (Unba-NL), Scenario 3 (Dis-NL), Scenario 4 (Sag-NL), and Scenario 5 (Swell-NL), implementation of FLC on UPQC supplied by PV without BES is able to result average THD of source voltage slightly better than PI controller and also limits prescribe in IEEE 519.

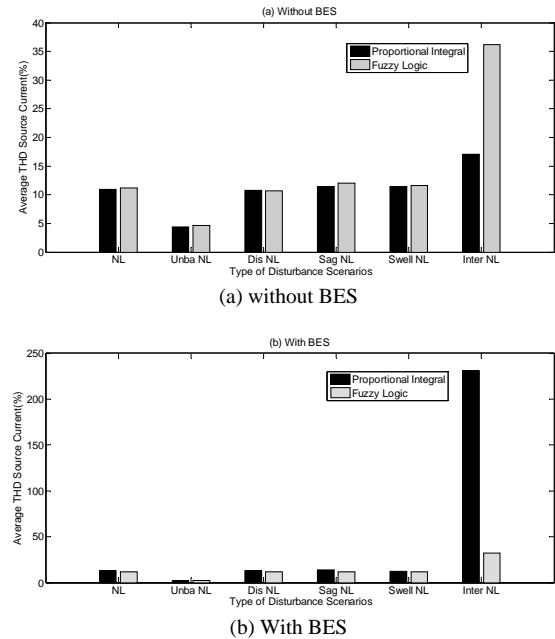
Otherwise under Scenario 6 (Inter-LN) PI controller gives better significantly result of average THD of  $V_L$  than FLC. Fig. 10(b) shows that in six scenarios, the use of FLC on UPQC supplied by PV with BES able to result average THD of  $V_L$  is slightly better than PI controller. In disturbance Scenarios 1 to 5, nominal of average THD of  $V_L$  has met IEEE 519. Otherwise under Scenario 6 (Inter-NL) FLC is able to reduce average THD of  $V_L$  significantly than PI controller.

Fig. 11(a) shows that in Scenario 1(NL), Scenario 2 (Unba-LN), Scenario 3 (Dis-NL), Scenario 4 (Sag-NL), and Scenario 5 (Swell-NL), the implementation of PI controller on UPQC supplied by PV without BES is able to result average THD of  $I_S$  slightly better than FLC.

Otherwise under Scenario 6 (Inter-LN) PI controller gives better significantly result of average THD of source voltage than FLC. Fig. 11(b) shows that in six scenarios, the use of FLC on UPQC supplied by PV with BES is able to give average THD of  $I_S$  better than PI controller.



Figs. 10. Performance of average THD of load voltage of UPQC supplied by PV using PI and FLC in six disturbance scenarios



Figs. 11. Performance of average THD of source current of UPQC supplied by PV using PI and FLC in six disturbance scenarios

Furthermore under Scenario 6 (Inter-NL), FLC is able to reduce average THD of source current significantly than PI controller.

#### IV. Conclusion

The use of BES supplied by PV connected to a three phase grid through to DC link of UPQC to improve power quality with PI controller and FLC have been discussed. In Scenario 6, PV is able to generate power to UPQC-DC link and injecting full average compensation voltage through injection transformer on series active filter so that average load voltage remains stable. During voltage interruption, even though there is low source current, combination of PV and BES is able to deliver power, store excess energy of PV, and inject compensation current into load bus through shunt active filter. The implementation of FLC on UPQC supplied PV with BES results average THD of load voltage slightly lower than using PI controller. In disturbance Scenarios 1 to 5, the implementation of FLC method UPQC supplied PV with BES is able to reduce the average THD of load voltage slightly better than PI controller and has already met the limits prescribed in IEEE 519. Otherwise under Scenario 6, FLC method is able to reduce average THD of load voltage significantly than PI controller. In disturbance scenarios 1 to 5, this method is able to give average THD of source current better than PI controller.

Furthermore under Scenario 6, it is also capable to give better performance significantly of average THD of source current more than PI controller.

Nevertheless, except under Scenario 2, the average THD of source current on UPQC supplied by PV without/with BES using FLC method still does not meet the limits prescribed in IEEE 519. Implementation of another Fuzzy Method i.e. Type 2 Fuzzy/Fuzzy Sliding Mode to control shunt active filter on UPQC is proposed as one solution to improve it.

#### Acknowledgements

The authors would like to acknowledge to Ministry of Research, Technology, and Higher Education, Republic of Indonesia, for financial support by BPP-DN Scholarships to pursue Doctoral Program in Department of Electrical Engineering, Faculty of Electrical Technology, ITS Surabaya.

#### References

- [1] B. Han, B. Hae, H. Kim, and S. Back, Combined Operation of Unified Power Quality Conditioner With Distributed Generation, *IEEE Transactions on Power Delivery*, Vol. 21, No. 1, pp. 330-338, January 2006.  
DOI: 10.1109/TPWRD.2005.852843
- [2] Vinod Khadkikar, Enhancing Electric Power Quality UPQC: A Comprehensive Overview, *IEEE Transactions on Power Electronics*, Vol. 27, No. 5, pp. 2284-2297, May 2012.  
DOI: 10.1109/TPEL.2011.2172001
- [3] Shafiuzzaman K. Khadem, Malabika Basu, and Michael F Conlon, Integration of UPQC for Power Quality Improvement in Distribution Generation Network, *ISGT Europe 2011*, Manchester, United Kingdom, December 2011.  
DOI: 10.1109/ISGTEurope.2011.6162813
- [4] Norshafinash Saudin, Junainah Ali Mohd Jobran, Muhammad Firdaus Mohd Isa, Mohd Azizi Mohamed, Latifah Mohamed and Surina Mat Suboh, Study on The Effect of Distributed Generation towards Unified Power Quality Conditioner Performance in Mitigating Voltage Sags, *IEEE International Conference on Power and Energy (PECon)*, 2-5 December 2012, Kota Kinabalu, Sabah, Malaysia, pp. 695-700.  
DOI: 10.1109/PECon.2012.6450304
- [5] S. N. Gohil, M. V. Makwana, K. T. Kadivar, G. J. Tetar, Three phase unified power quality conditioner (UPQC) for power quality improvement by using UVTG technique, *2013 International Conference on Renewable Energy and Sustainable Energy (ICRESE)*, 5-6 Dec. 2013, pp 151 – 156, Coimbatore, DOI: 10.1109/ICRESE.2013.6927805
- [6] Yahia Bouzelata, Erol Kurt, Rachid Chenni, Necmi Altin, Design and Simulation of Unified Power Quality Conditioner Fed by Solar Energy, *International Journal of Hydrogen Energy* 40, 15267-15277, pp. 15267-15277, Elsevier Ltd, 2015.  
DOI: <http://dx.doi.org/10.1016/j.ijhydene.2015.02.077>
- [7] Jayachandran, R. Murali Sachithanandam, Performance Investigation of Unified Power Quality Conditioner Using Artificial Intelligent Controller, *International Review on Modelling Simulation (IREMOS)*, Vol 8, No 1. (2015).  
DOI: <https://doi.org/10.15866/iremos.v8i1.5396>
- [8] K.Ramalingeswara Rao, K.S. Srikanth, Improvement of Power Quality using Fuzzy Logic Controller In Grid Connected Photovoltaic Cell Using UPQC", *International Journal of Power Electronics and Drive System (IJPEDS) Vol. 5, No. 1, July 2014*, pp. 101-111 ISSN: 2088-8694.  
DOI: <http://dx.doi.org/10.11591/ijpeds.v5i1.6184>
- [9] Amirullah, Mochamad Ashari, Ontoseno Penangsang, Adi Soeprijanto, Multi Units of Single Phase Distributed Generation Combined With Battery Energy Storage for Phase Balancing in Distribution Network, *UTM Jurnal Teknologi* Vol. 78: 10-4 (2016), pp. 27-33, eISSN 2180-3722, Universiti Teknologi Malaysia (UTM) Publisher.  
DOI: <https://doi.org/10.11113/jt.v78.9887>
- [10] K.S. Srikanth, Krishna Mohan T, P. Vishnuvardhan, Improvement of Power Quality for Microgrid Using Fuzzy Based UPQC Controller, *International Conference on Electrical, Electronics, Signals, Communication and Optimization (EESCO), 2015 Visakhapatnam*, pp. 1-6, 24-25 Jan. 2015.  
DOI: 10.1109/EESCO.2015.7253882
- [11] Ali Reza Reisi, Muhammad H. Moradi, Hemen Showkati, Combined Photovoltaic and Unified Power Quality Controller to Improve Power Quality, *Solar Energy* 88 (2013), pp.154-162.  
DOI: <https://doi.org/10.1016/j.solener.2012.11.024>
- [12] Yash Pal, A. Swarup, Bhim Singh, A Comparative Analysis of Different Magnetic Support Three Phase Four Wire Unified Power Quality Conditioners – A Simulation Study, *Electrical Power and Energy System* 47 (2013), pp. 437-447.  
DOI: <https://doi.org/10.1016/j.ijepes.2012.11.014>
- [13] Swapnil Y. Kamble, Madhukar M. Waware, Unified Power Quality Conditioner for Power Quality Improvement, *2013 International Multi Conference on Automation, Computing, Communication, Control and Compressed Sensing (iMac4s)*, pp. 432-437, Kottayam, India, 22-23 March 2013.  
DOI: 10.1109/iMac4s.2013.6526450
- [14] Mihir Hembram, Ayan Kumar Tudu, Mitigation of Power Quality Problems Using Unified Power Quality Conditioner (UPQC), *Proceedings of the 2015 Third International Conference on Computer, Communication, Control and Information Technology (C3IT)*, (2015), pp.1-5, Hooghly, India, 7-8 Feb. 2015.  
DOI: 10.1109/C3IT.2015.7060174
- [15] Amirullah, Agus Kiswantono, Power Quality Enhancement of Integration Photovoltaic Generator to Grid under Variable Solar Irradiance Level using MPPT-Fuzzy, *International Journal of Electrical and Computer Engineering (IJECE)*, IAES Publisher, Vol. 6, No. 6, December 2016, ISSN: 2088-8708.



DOI: <http://dx.doi.org/10.11591/ijece.v6i6.12748>

- [16] Brusco, G., Burgio, A., Menniti, D., Pinnarelli, A., Sorrentino, N., About the Effectiveness, the Electric Demand Profile Impact and the Imbalance Reduction of an Optimal Sized CHP Generator for an Agro-Industrial Microgrid Using Real Data, (2015) *International Review of Electrical Engineering (IREE)*, 10 (3), pp. 362-369.  
doi:<https://doi.org/10.15866/iree.v10i3.5709>
- [17] Kerdphol, T., Qudaih, Y., Hongesombut, K., Watanabe, M., Mitani, Y., Intelligent Determination of a Battery Energy Storage System Size and Location Based on RBF Neural Networks for Microgrids, (2016) *International Review of Electrical Engineering (IREE)*, 11 (1), pp. 78-87.  
doi:<https://doi.org/10.15866/iree.v11i1.7718>
- [18] Tephirik, N., Hongesombut, K., Enhancement of Stabilizing Performance of a Microgrid Using Energy Storage System with Under Frequency Relay, (2016) *International Review of Electrical Engineering (IREE)*, 11 (6), pp. 635-643.  
doi:<https://doi.org/10.15866/iree.v11i6.10342>
- [19] Jayachandran, J., Murali Sachithanandam, R., Artificial Intelligence Based Controller for Series and Shunt Active Filters for Power Quality Improvement, (2015) *International Review of Automatic Control (IREACO)*, 8 (3), pp. 180-190.  
doi:<https://doi.org/10.15866/ireaco.v8i3.5942>



**Adi Soeprijanto** was born in Lumajang East Java Indonesia, in 1964. He received bachelor in electrical engineering from ITB Bandung, in 1988. He received master of electrical engineering in control automatic from ITB Bandung. He continued his study to Doctoral Program in Power System Control in Hiroshima University Japan and was finished in 2001. He is currently a professor at Department of Electrical Engineering and member of PSSL in ITS Surabaya. His main interest includes power system analysis, power system stability control, and power system dynamic stability. He had already achieved a patent in optimum operation of power system.

## Authors' information

<sup>1</sup>Department of Electrical Engineering, Faculty of Electrical Technology, Institut Teknologi Sepuluh Nopember (ITS) Surabaya, Study Program of Electrical Engineering, Faculty of Engineering, University of Bhayangkara Surabaya, Indonesia.  
E-mails: [amirullah14@mhs.ee.its.ac.id](mailto:amirullah14@mhs.ee.its.ac.id)  
[amirullah@ubhara.id](mailto:amirullah@ubhara.id)

<sup>2</sup>Department of Electrical Engineering, Faculty of Electrical Technology, ITS Surabaya, Indonesia.  
E-mails: [ontosenop@ee.its.ac.id](mailto:ontosenop@ee.its.ac.id)  
[Zenno\\_379@yahoo.com](mailto:Zenno_379@yahoo.com)  
[adisup@ee.its.ac.id](mailto:adisup@ee.its.ac.id)



**Amirullah** was born in Sampang East Java Indonesia, in 1977. He received bachelor and master degree in electrical engineering from University of Brawijaya Malang and ITS Surabaya, in 2000 and 2008, respectively. He also worked as a lecturer in University of Bhayangkara Surabaya. He is currently working toward the doctoral degree, in electrical engineering in Power System and Simulation Laboratory (PSSL) ITS Surabaya His research interest includes power distribution modeling and simulation, power quality, harmonics mitigation, design of filter/PFC, and renewable energy



**Ontoseno Penangsang** was born in Madiun East Java Indonesia, in 1949. He received bachelor degree in electrical engineering from ITS Surabaya, in 1974. He received M.Sc and Ph.D degree in Power System Analysis from University of Wisconsin, Madison, USA, in 1979 and 1983, respectively. He is currently a professor at Department of Electrical Engineering and the head of PSSL ITS Surabaya. He has a long experience and main Interest in power system analysis (with renewable energy sources), design of power distribution, power quality, and harmonic mitigation in industry.